Voltage-dependent processes in the electroneutral amino acid exchanger ASCT2

Catherine B. Zander, Thomas Albers, and Christof Grewer

Department of Chemistry, Binghamton University, Binghamton, NY 13902

Neutral amino acid exchange by the alanine serine cysteine transporter (ASCT)2 was reported to be electroneutral and coupled to the cotransport of one Na^+ ion. The cotransported sodium ion carries positive charge. Therefore, it is possible that amino acid exchange is voltage dependent. However, little information is available on the electrical properties of the ASCT2 amino acid transport process. Here, we have used a combination of experimental and computational approaches to determine the details of the amino acid exchange mechanism of ASCT2. The [Na^+] dependence of ASCT2-associated currents indicates that the Na^+/amino acid stoichiometry is at least 2:1, with at least one sodium ion binding to the amino acid–free *apo* form of the transporter. When the substrate and two Na^+ ions are bound, the valence of the transport domain is +0.81. Consistently, voltage steps applied to ASCT2 in the fully loaded configuration elicit transient currents that decay on a millisecond time scale. Alanine concentration jumps at the extracellular side of the membrane are followed by inwardly directed transient currents, indicative of translocation of net positive charge during exchange. Molecular dynamics simulations are consistent with these results and point to a sequential binding process in which one or two modulatory Na^+ ions bind with high affinity to the empty transporter, followed by binding of the amino acid substrate and the subsequent binding of a final Na^+ ion. Overall, our results are consistent with voltage-dependent amino acid exchange occurring on a millisecond time scale, the kinetics of which we predict with simulations. Despite some differences, transport mechanism and interaction with Na^+ appear to be highly conserved between ASCT2 and the other members of the solute carrier 1 family, which transport acidic amino acids.

The Journal of General Physiology

INTRODUCTION

The amino acid transporter alanine serine cysteine transporter (ASCT)2 transports small, neutral amino acids across the membrane in exchange with intracellular amino acids (Utsunomiya-Tate et al., 1996; Bröer et al., 1999, 2000; Bode, 2001). ASCT2 belongs to the solute carrier 1 (SLC1) family of transporters. The structure of a bacterial glutamate transporter homologue of ASCT2 (glutamate transporter homologue from *Pyrococcus horikoshii* [GltPh]) is known in complex with the transported amino acid substrate (aspartate) and two sodium ions (Yernool et al., 2004; Boudker et al., 2007). Considering the high similarity of the amino acid sequence in the transmembrane domains, it is reasonable to assume that the ASCT2 structure is based on the same fold as that of the glutamate transporters (Albers et al., 2012).

Despite this homology with the glutamate transporters, which have been much more thoroughly studied, the functional properties of the ASCTs are not very well established. For example, the coupling stoichiometries of Na^+ and amino acid in system ASC (transport system that prefers alanine, serine, and cysteine) and ASCT2 are unknown, although models with a 1:1 ratio have been proposed (Bussolati et al., 1992; Bröer et al., 2000; Grewer and Grabsch, 2004). However, mammalian glutamate transporters cotransport three Na^+ ions with one glutamate molecule (Zerangue and Kavanaugh, 1996b), raising the possibility that the stoichiometry of ASCT2 amino acid exchange is also more complex than 1 amino acid: 1 Na^+ ion. Furthermore, amino acid exchange by system ASC and ASCT2 was proposed to be electroneutral (Valdeolmillos et al., 1986; Utsunomiya-Tate et al., 1996), whereas transport by the second ASCT subtype, ASCT1, was proposed to be electrogenic (Zerangue and Kavanaugh, 1996a). Because the amino acid is most likely transported in its zwitterionic, net neutral form, the cotransport of the positively charged sodium ions may lead to at least partial electrogenicity of ASCT2 transport (Bussolati et al., 1992). However, electrogenic reaction steps in ASCTs have not yet been identified.

In this paper, we characterized the mechanism of sodium interaction with ASCT2 and identified the voltage dependence of amino acid exchange. Using a computational approach, based on continuum electrostatic Poisson–Boltzmann (PB) theory, we estimated the net

Correspondence to Christof Grewer: cgrewer@binghamton.edu

Abbreviations used in this paper: APBS, adaptive Poisson–Boltzmann solver; ASCT, alanine serine cysteine transporter; EAAT, excitatory amino acid transporter; GltPh, glutamate transporter homologue from *Pyrococcus horikoshii*; MD, molecular dynamics; MNI, methoxynitroindoline; PB, Poisson–Boltzmann; RL2, reentrant loop 2; SLC1, solute carrier 1.

The Rockefeller University Press $30.00
J. Gen. Physiol. Vol. 141 No. 6 659–672
www.jgp.org/cgi/doi/10.1085/jgp.201210948

charge translocation of ASCT2 with various numbers of cations bound, predicting that the main translocation reaction is associated with the movement of positive charge across the membrane. Consistent with this prediction, charge movement was observed experimentally by applying step changes in the membrane potential, or alanine concentration jumps to ASCT2. In addition, we obtained experimental evidence that at least two Na^+ ions are cotransported with amino acid. Results from molecular dynamics (MD) simulations also suggest the existence of at least two, possibly three, Na^+-binding sites. Our results are explained with a sequential transport mechanism in which one Na^+ binds to the empty transporter, followed by binding of the amino acid and the subsequent binding of another Na^+ ion, followed by electrogenic amino acid translocation across the cell membrane.

MATERIALS AND METHODS

Cell culture and transfection

cDNA coding for rat ASCT2 was provided by S. Bröer (The Australian National University, Acton, Australia; Bröer et al., 1999, 2000). The coding region of the cDNA was subcloned into the EcoRI site of the pBK-CMV vector (Agilent Technologies). The cDNA construct was used to transiently transfect human embryonic kidney (HEK) cells (HEK293; American Type Culture Collection no. CGL 1573) with reagent (Fugene HD; Roche), according to the instructions of the supplier. Cells were transfected in the exponential growth phase. Electrophysiological experiments were done 24 h after transfection.

Electrophysiological methods

ASCT2-mediated currents were recorded with an amplifier (Adams and List EPC7; HEKA) under voltage-clamp conditions. The whole-cell current-recording configuration was used. Electrode resistances were 2–3 MΩ, and the series resistance (R_S) was 5–8 MΩ. R_S was not compensated in the steady-state recordings, as compensation had no effect on the magnitude of the observed currents. However, up to 60% R_S compensation was used in the voltage-jump experiments to accelerate the time needed for charging of the membrane. We have previously estimated the instrument time constant under these conditions as 200 µs (Mim et al., 2007). The extracellular bath solution contained (mM): 140 NaMES or NaSCN, 2 Mg gluconate$_2$, 2 Ca gluconate$_2$, and 10 HEPES (MES, pH 7.4/NaOH). The pipette solution contained (mM): 130 NaMES or NaSCN, 2 $MgCl_2$, 10 EGTA, 10 HEPES, and 10 liter-alanine/cysteine, pH 7.3/NaOH. Using this intracellular solution, the transporters operate in the exchange mode, in which external amino acid is exchanged with internal amino acid in the absence of net transport. The exchange mode is associated with the activation of an uncoupled anion current, which was used to determine the $[Na^+]$ dependence. For experiments in the presence of intracellular K^+, Na^+ in the above solutions was replaced with K^+. For $[Na^+]$-dependent experiments, Na^+ was replaced with *N*-methylglucamine$^+$ (NMG^+). The currents were low-pass filtered at 3 kHz (EPC7 built-in filter) and digitized with a digitizer board (Digidata 1200; Axon Instruments) at a sampling rate of 10–50 kHz (controlled by Axon PClamp7 software). All experiments were performed at room temperature.

Rapid solution exchange was essentially performed as described previously (Watzke et al., 2001). In brief, substrates and inhibitors were applied to the ASCT2-expressing HEK293 cells with a quartz tube (350-µm tube diameter) positioned at a distance of ≈0.5 mm to the cell. The linear flow rate of the solutions emerging from the opening of the tube was ∼5–10 cm/s, resulting in typical rise times of the whole-cell current of 30–50 ms (10–90%).

Laser-pulse photolysis

Laser-pulse photolysis experiments were performed as described previously (Zhang et al., 2007). In brief, the cells were equilibrated with neutral amino acids or methoxynitroindoline (MNI)-caged alanine using a fast solution exchange device. Photolysis was initiated with a light flash generated by a frequency-tripled Nd-Yag laser (Minilite II; Continuum). The laser light was delivered to the cell with an optical fiber (350-µm diameter), and its energy was adjusted with neutral density filters (Andover Corporation). Typical laser energies, measured at the emitting end of the optical fiber using an energy meter (Gentec), were in the range of 50 to 400 mJ/cm^2. A standard alanine concentration of 1 mM was applied to the cell by rapid solution exchange before and after laser-pulse photolysis to estimate the concentration of photolytically released alanine and to test the cell for damage by the laser pulse.

Data analysis

Nonlinear regression fits of experimental data were performed with Origin (OriginLab) or Clampfit (pClamp8 software; Axon Instruments). Dose–response relationships of currents were fitted with a Michaelis–Menten-like equation, yielding K_m and I_{max}. Each experiment was performed in triplicate with at least two different cells. The error bars represent mean ± SD, unless stated otherwise.

PB calculations using adaptive PB solver (APBS)mem

Calculations of electrostatic energies were essentially performed as described previously (Grewer et al., 2012). The parameters for the APBSmem routine (Callenberg et al., 2010) were as follows. The temperature was set to 298 K. The symmetrical ion concentrations were set to 0.1 M. The membrane thickness was 30 Å, with an upper and lower exclusion radius of 31 and 23 Å, respectively. The dielectric constants were 80 for the intracellular and extracellular water and within the extracellular bowl created within the exclusion radius, 2.0 for the membrane, and 2–10 for the protein. The lipid headgroup region of the bilayer was not modeled. For the PB calculations, the finest focusing step used 161 grid points, in a 130-Å grid, in x, y, and z directions. Three focusing steps were used, and with these parameters the energy values converged. The C and N termini were charged. Neutralization of the termini only has a minor effect on the results. To assess the effect of the *z*-position within the membrane, the transporter was moved up and down by ±2 Å relative to the membrane. This caused a reduction of the calculated valence by 21–25% but in no case changed the sign of the valence.

MD simulation protocol

The simulated system consists of the trimeric ASCT2 transporter, modeled on the structure of the GltPh transporter (Protein Data Bank accession nos. 2NWX [Boudker et al., 2007] and 3KBC [Reyes et al., 2009]; sequence alignment shown in Fig. S1), set up in a patch of POPE membrane in its box of water using visual MD (Humphrey et al., 1996). The overall system (neutralized by adding counterions) is composed of ∼13,3000 atoms (illustrated in Fig. S2). The Modeller algorithm was used to build the homology model (Eswar et al., 2003). The C- and N-terminal domains of ASCT2 are not present in the GltPh crystal structures. Therefore, the ASCT2 sequence was truncated before V56 (N terminus) and after T487 (C terminus). The simulation uses the CHARMM27 force field with the CMAP corrections and the TIP3P model for explicit water. MD calculations were performed with periodic boundary conditions with a time step of 2 fs using NAMD 2.8

(Phillips et al., 2005). First, lipid tails were melted while all other atoms were held fixed for 400 ps at constant volume and constant temperature of 300 K. Then, the system was equilibrated at constant temperature and constant pressure of 1 bar for 500 ps while the atoms of the protein were restrained by harmonic potentials (k = 1 kcal/mol/Å^2) to allow for packing of the lipid molecules around the protein. Next, the simulation was continued for 1 ns without constraints.

Production runs of up to 12 ns were performed after 8 ns of equilibration at constant area of the lipid bilayer and at constant pressure of 1 bar. Constant temperature was maintained by using Langevin dynamics with a damping coefficient of 5 ps. The Langevin piston method was used to maintain a constant pressure of 1.0 atm with a piston period of 200 fs. Short-range nonbonded interactions were calculated using a cutoff distance of 12 Å, and long-range electrostatic interactions were calculated using the particle mesh Ewald method (Darden et al., 1993).

Online supplemental material

The online supplemental material contains tables showing data from PB calculations (Tables S1 and S2), the sequence alignment between ASCT2 and GltPh for homology modeling (Fig. S1), an illustration of the MD setup (Fig. S2), and additional results from MD simulations (Fig. S3). The online supplemental material is available at http://www.jgp.org/cgi/content/full/jgp.201210948/DC1.

RESULTS

One or two sodium ions bind to the *apo* form of the transporter

Previous results showed that Na^+ can activate a leak anion conductance in the amino acid–free *apo* form of ASCT2 (Grewer and Grabsch, 2004). In agreement with these results, anion current induced by Na^+ in the absence of amino acid was activated at low [Na^+] (Fig. 1), with an apparent K_m of 0.25 ± 0.06 mM. High [Na^+], however, led to a small but significant reduction of the anion current (K_m estimated as 51 mM, although an exact value cannot be determined because of lack of saturation at 140 mM Na^+; Fig. 1). This biphasic behavior can be explained by the binding of at least one but possibly two Na^+ ions to the *apo* form of the transporter (see fit to two-site model in Fig. 1). In this interpretation, [Na^+] below 5 mM results in occupation of only the first high affinity binding site with an apparent K_m of 0.25 mM and activation of the leak anion conductance. The intrinsic dissociation constant of this binding step will be termed "K_{Na1}" throughout this paper. At [Na^+] of 140 mM and higher, the low affinity binding site with an apparent K_m in the 50-mM range is also occupied, resulting in a state with two Na^+ ions bound. This state has slightly lower anion conductance than the singly occupied state, causing the reduction of the leak anion current at high [Na^+] in Fig. 1.

ASCT2 harbors at least two Na^+-binding sites

It has been hypothesized that amino acid transport by ASCT2 is coupled to the exchange of one Na^+ ion (Bussolati et al., 1992; Bröer et al., 2000; Grewer and Grabsch, 2004). However, the highly homologous bacterial aspartate transporter GltPh has two identified Na^+-binding sites (cotransporting three Na^+ ions; Boudker et al., 2007; Groeneveld and Slotboom, 2010), and mammalian glutamate transporters may have three Na^+ sites (Zerangue and Kavanaugh, 1996b). To test for potential multiple Na^+-binding sites, we determined the Na^+ dependence of ASCT2 function. This was done using the well-established anion conductance of ASCT2 as a readout (Grewer and Grabsch, 2004), as this conductance can be activated in the exchange mode at steady state. Fig. 2 A shows anion currents at various extracellular [Na^+]. The current was inwardly directed at high [Na^+], as expected from an alanine-induced activation of the anion conductance (SCN^- outflow). At [Na^+] below 2 mM, the leak anion current was reduced after the application of alanine (Fig. 2 A). This apparent outward current was induced by alanine inhibition of the tonic leak anion conductance, resulting in inhibition of SCN^- outflow (see Grewer and Grabsch, 2004). This current–[Na^+] relationship is quantified in Fig. 2 B. The outward current at low [Na^+] indicates that alanine is an inhibitor of the leak anion conductance under these conditions, as previously found for competitive ASCT2 inhibitors (Albers et al., 2012). This biphasic [Na^+] dependence of the anion current is incompatible with a single-Na^+ site model but clearly requires the existence of at least two Na^+-binding sites. Furthermore, our data show that low sodium concentration cannot be overcome by saturating [alanine], directly demonstrating that at least one Na^+ ion must bind to the alanine-bound form of the transporter.

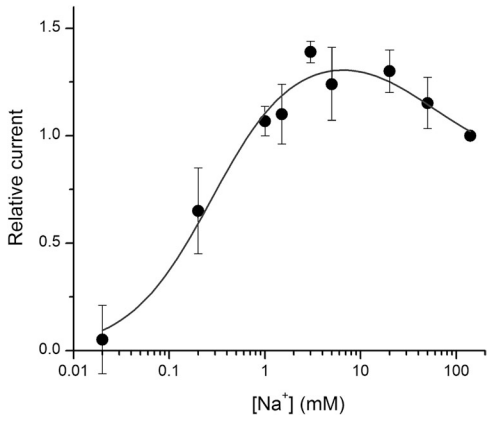

Figure 1. At least one but possibly two Na^+ ions bind to the *apo* form of ASCT2. [Na^+] dependence of the leak anion current (normalized to the response at 140 mM Na^+). The solid line represents a fit to the equation $I = A\,[Na^+]/(K_1 + [Na^+]) + B\,[Na^+]/(K_2 + [Na^+])$. Here, A and B are scaling parameters, and the values for K_1 and K_2 were 0.25 ± 0.06 mM and 51 ± 10 mM, respectively. The intracellular solution contained 120 mM NaSCN and 10 mM alanine. The extracellular solution contained 140 mM NaMes (V = 0 mV).

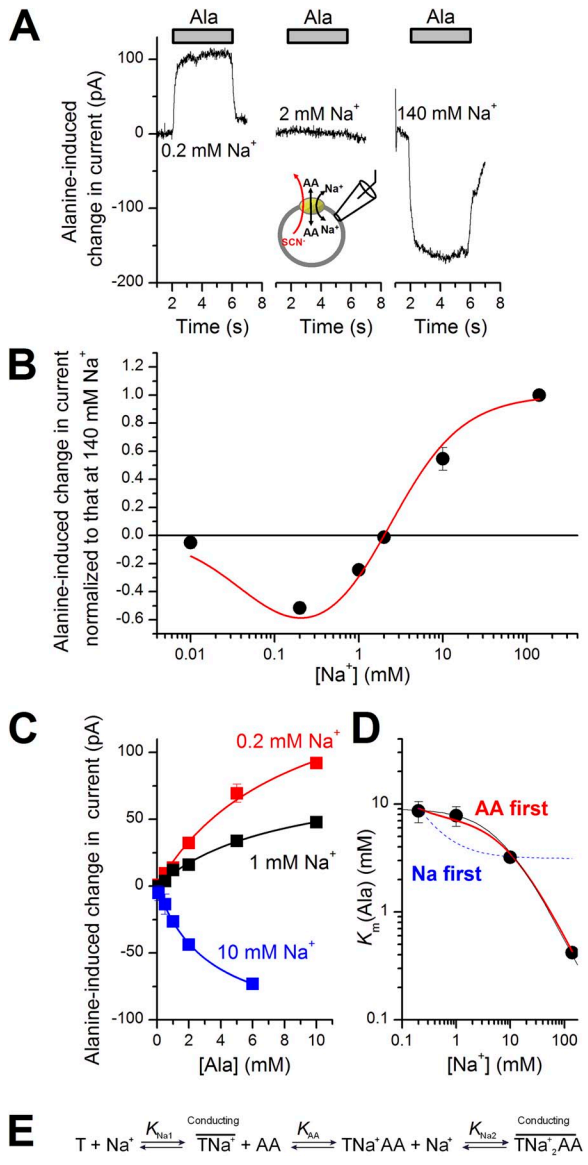

Figure 2. Direct evidence for two ASCT2 Na^+-binding sites. (A) Original anion current recordings upon the application of 10 mM alanine (timing indicated by the bars) at $[Na^+]$ of 0.2 mM (left), 2 mM (middle), and 140 mM (right). The membrane potential was 0 mV, and the pipette solution contained 140 mM NaSCN and 10 mM alanine. The external anion was Mes^-. Na^+ was replaced by NMG^+. (B) $[Na^+]$ dependence of the maximum alanine-induced current, I_{max}, at saturating [alanine] (V = 0 mV, normalized to the current at 140 mM Na^+). The solid line represents a fit of Eq. 8 (see Appendix), assuming a two-site binding model. The fitted parameters are: K_{Na1} = 0.1 mM, K_{Na1} = 2.8 mM, and r = 1.9. (C) Determination of the K_m of ASCT2 for alanine at different $[Na^+]$. The solid lines represent fits to a Michaelis–Menten-type equation. (D) Dependence of the K_m for alanine on $[Na^+]$. The solid red line represents a fit using the equation $K_m = (1 + K_{Na1}/[Na^+])K_S/(1 + [Na^+]/K_{Na2})$ (Eq. 9; see Appendix), assuming a two-site binding model (K_{Na1} = 0.1 mM, K_{Na2} = 8.5 mM, and K_S = 7.5 mM; K_{Na1} was fixed in the fitting procedure). The dashed blue line represents a model in which two $[Na^+]$ bind before the amino acid (Eq. 10; see Appendix). The black solid line represents a model in which only alanine binding and one subsequent Na^+-binding step were included ($K_m = K_S/(1 + [Na^+]/K_{Na2})$, K_{Na2} = 6.5 mM, and K_S = 9 mM). (E) Minimal sequential mechanism for Na^+ and amino acid (AA) binding to the transporter, T. The bars illustrate the anion-conducting states.

Fig. 2 C shows the [alanine] dependence of the anion current at various $[Na^+]$, which we used to determine the K_m for alanine. The K_m for alanine decreased with increasing sodium concentration (Fig. 2 D). Although this $[Na^+]$ dependence is not consistent with a model in which Na^+ binds only to the alanine-free transporter (Fig. 2 D, blue, dashed line), it can be fit with a model in which one Na^+ binds to the empty transporter and one Na^+ binds to the alanine-loaded transporter (Fig. 2 D, red, solid line; see Appendix for equations). Together with our data on the $[Na^+]$ dependence of I_{max}, these results show unequivocally that at least one Na^+ ion must bind to the substrate-bound form of ASCT2. A minimal kinetic model that can explain the Na^+-binding data is shown in Fig. 2 E.

The amino acid exchange reaction is associated with charge movement

If the major conformational transition resulting in amino acid exchange is electrogenic, steps in the transmembrane potential should result in relaxation to a new exchange equilibrium. Consistent with this prediction, steps in the membrane potential applied to ASCT2 in voltage-clamped cells induce transient current in the presence of amino acid, but not in its absence (Fig. 3 B; voltage protocol is shown in Fig. 3 A). By subtracting these two currents from each other, the specific, amino acid–sensitive current was obtained. As shown in Fig. 3 C, no steady-state component was observed, as expected for an equilibrium exchange process in the absence of any net driving force. The transient currents appeared to be capacitive in nature, because the charge moved in the inward direction upon application of negative potential was identical in magnitude but of opposite sign to the charge moved after reverting the voltage to its original value (Fig. 3, B and C). The charge movement was voltage dependent (Fig. 3 D) and could be fit with the Boltzmann equation, yielding an apparent valence of $z_Q = 0.74 \pm 0.14$ (n = 3). The transient current decayed with a time constant of 1.6 ± 0.3 ms at 0 mV, indicating that relaxation of the exchange equilibrium is rapid. The relaxation rate constant was weakly dependent on the transmembrane potential (Fig. 3 E), with an apparent valence of ∼0.42.

We performed control experiments to test whether the voltage jump–induced charge movement is specifically mediated by ASCT2. The transient currents in the presence of amino acid were inhibited by the competitive ASCT2 inhibitors serine fluorenylcarboxylic acid ester (Albers et al., 2012) and benzylserine (Grewer and

Grabsch, 2004; unpublished data). Furthermore, no amino acid–sensitive currents were detected in non-transfected control cells.

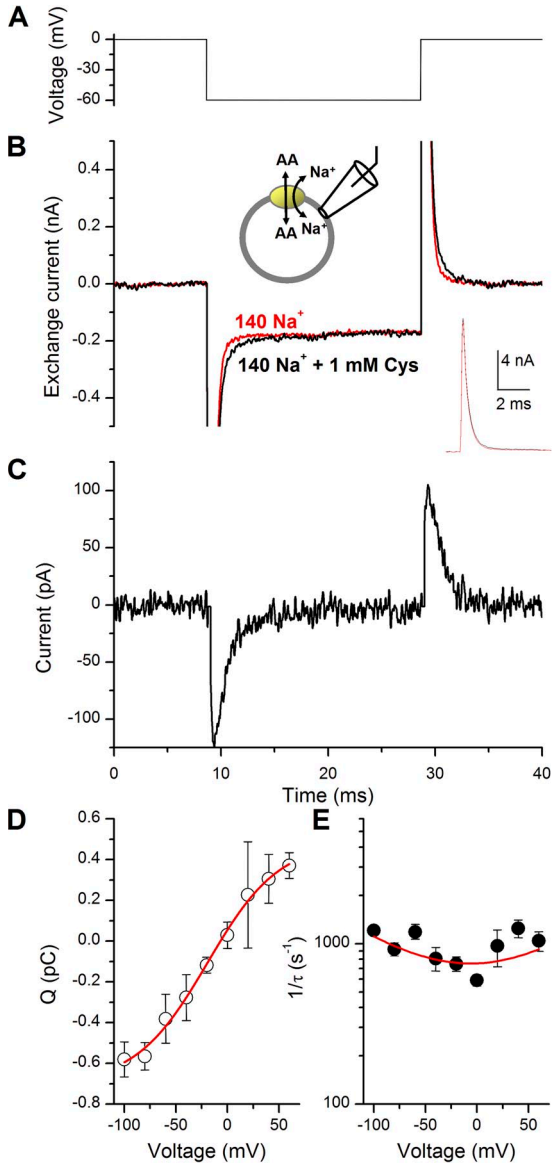

Figure 3. Amino acid exchange by ASCT2 is associated with transmembrane charge movement. (A) Voltage-jump protocol used in the experiment. (B) Original current traces in response to the voltage jump in the absence (red) and presence (black) of 1 mM cysteine (inset shows original currents not cut off at 0.5 nA). (C) Current trace obtained by subtraction of currents in the presence from that in the absence of cysteine. (D) Voltage dependence of the charge movement of the on-response obtained by integrating the current over time. The red line illustrates a fit of the Boltzmann equation ($Q(V_m) = Q_{min} + Q_{max} \cdot [1 + \exp(Z_Q(V_Q - V_m) \cdot F/(RT))]^{-1}$; Q represents the charge moved, Z_Q is the valence of this charge, V_Q is the midpoint potential of the charge movement, R is the gas constant, T is the temperature, and F is the Faraday constant) to the data with a z_q of 0.74 and a midpoint potential of −19 mV. (E) Voltage dependence of the relaxation rate constant for decay of the transient current. The line represents a fit to the equation $1/\tau = k_1(0) \exp(z_qFV/2RT) + k_2(0) \exp(-z_qFV/2RT)$, with $z_q = 0.41$.

Continuum electrostatic models predict electrogenic nature of ASCT2 conformational transitions

To rationalize the results from the voltage-jump experiments, we used a computational approach to predict valences associated with the ASCT2 exchange reaction. The approach is based on solving the linearized PB equation for different structural states of the transporter in the presence of an internal biasing potential. The APBS was used for the calculations (Baker et al., 2001). If two states of a membrane protein are connected by an electrogenic transition, one state should be stabilized by the transmembrane potential relative to the other in terms of its total electrostatic energy (Callenberg et al., 2010). This approach has been successfully applied in the past to voltage-gated ion channels (Grabe et al., 2004; Silva et al., 2009; Choudhary et al., 2010). The setup of the system, using an implicit membrane with dielectric constant $\varepsilon = 2$, is shown in Fig. 4 A. The transport proteins, which are homology models of ASCT2 based on the GltPh structures (Protein Data Bank

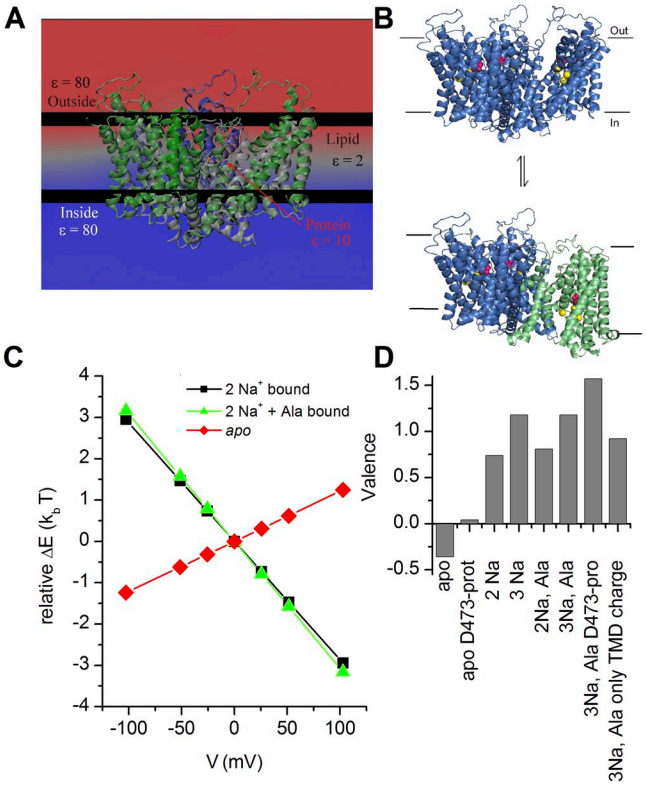

Figure 4. Valence associated with transitions of several forms of the ASCT2 transport domain. (A) Setup used for the APBS calculations. Blue color indicates inside positive or negative membrane potential (+ or −100 mV), and red color indicates 0-mV membrane potential. (B) Illustration of the conformational change of an individual transport domain from outward- to inward-facing. (C) Relative change in the total electrostatic energy for the outward-facing to inward-facing transition of an individual subunit for the *apo* transporter (red), and the forms with 2 Na^+ bound (black) and 2 Na^+ and alanine bound (ΔE was set to 0 k_bT at 0 mV). (D) Valences calculated from the slopes of C.

accession nos. 2NWX [Boudker et al., 2007] and 3KBC [Reyes et al., 2009]), were inserted into the membrane using the APBSmem routine (Callenberg et al., 2010).

We first determined the valence of what is thought to be the major conformational transition from outward- to inward-facing configuration (Fig. 4, A and B; Crisman et al., 2009; Reyes et al., 2009). As illustrated in Fig. 4 (C and D), inside negative potential slightly stabilized the outward-facing configuration in the empty transporter (valence, $z = -0.35$), suggesting that in the absence of bound cations, the transporter carries a net negative charge (assuming pK_a values for the buried charges to be similar to their pK_a values in water). The addition of cations to their presumed binding sites (modeled in analogy to the Na1 and Na2 sites of GltPh; see below) resulted in a positive valence of this transition (Fig. 4, B and C). As expected, the overall neutral zwitterionic amino acid substrate (alanine) contributed only minimally to the valence (Fig. 4, C and D). Glutamate transporters have a third Na^+-binding site, which was proposed to be formed by conserved amino acid side chains deeply buried within the transmembrane domain (for example, D367 and T101; Tao et al., 2006, 2010; Huang and Tajkhorshid, 2010). These amino acid residues are conserved in ASCT2. Thus, it is possible that ASCT2 harbors a third Na^+-binding site in this position. After adding a third Na^+ ion to this site, the valence of the loaded transporter was calculated as $z = +1.18$ (Fig. 4 D). The results of the PB calculations are summarized in Table S1. Fig. 4 D also shows results from control PB calculations in which all charges but seven conserved ones in the transmembrane domain were removed to test for contribution of the movement of charges in the soluble domain of the transporter to the valence. Although the valence was slightly reduced after removal of these charges, the sign of the valence was unchanged (Fig. 4 D). Collectively, our continuum electrostatic analysis suggests that the transition from the outward- to the inward-facing state is associated with positive charge movement in the amino acid/Na^+-loaded transporter and is, thus, electrogenic.

Ionizable amino acid residues deeply buried in the transmembrane domain may have perturbed pK_a values, as recently suggested for the aspartate side chain coordinating sodium in the Na1 site of glutamate transporters (Mwaura et al., 2012). To test this hypothesis, we estimated pK_a values of relevant side chains using the empirical PROPKA approach (Rostkowski et al., 2011). The estimated values suggest that at least D473, which is expected to contribute to Na^+ binding, has a strongly elevated pK_a (10.3 outward-facing, 10.9 inward facing) in the absence of ions. Assuming that the D473 side chain is protonated, the valence of the conformational transition of the *apo* form of ASCT2 is +0.05 and that of the fully loaded form (3 Na^+ and Ala) is +1.57 (Fig. 4 D).

Rapid application of amino acid induces transient currents caused by relaxation of the electrogenic exchange equilibrium

The exchange equilibrium can be perturbed by voltage jumps as well as by rapid application of amino acid. In this single-turnover experiment, the transporter-binding sites are initially distributed according to the equilibrium constant associated with the inward-outward–facing transition in the absence of amino acid. When amino acid is rapidly applied to the extracellular side, binding to ASCT2 initiates transition to the inward-facing configuration. A typical current recording is shown in Fig. 5 B in the presence of intracellular K^+, a cation that is not thought to interact with ASCT2. Rapid alanine application through photolysis of caged alanine (Zhang et al., 2007) within less than a microsecond (Fig. 5 A; released [alanine], ~600 µM) resulted in a small transient inward current that rapidly relaxed back to a steady state within ~10 ms (Fig. 5 B). The inward direction of the current proves that positive charge is moving into the cell during the exchange equilibration process. Control experiments with nontransfected cells demonstrate the absence of current signals upon application of the laser flash. Further control experiments are shown in Zhang et al. (2007).

The observed time constant associated with the current decay, $\tau_{obs} = 1/k_{obs}$, can be analyzed using the simplified kinetic scheme (Scheme 1) shown in the Appendix. According to this scheme, the equation for k_{obs} is:

$$k_{obs} = k_1 + k_{-1}. \quad (1)$$

In the presence of intracellular K^+, τ_{obs} was 3.1 ± 0.5 ms. As expected, no steady-state current was observed because ASCT2 is incapable of catalyzing steady-state forward transport. According to Eq. 1, $k_{obs} = k_1$ under these conditions because the reverse reaction (T_{in} to T_{out}) cannot be initiated in the absence of internal Na^+ and amino acid ($k_{-1} = 0$).

To further analyze the exchange reaction, we repeated the experiment under exchange conditions (140 mM Na^+ and 10 mM alanine inside, rather than K^+). Here, binding sites initially face outward (state T_{out} in Scheme 1; see Appendix), caused by the application of high amino acid and Na^+ concentrations to the intracellular side in the absence of extracellular amino acid (Fig. 5 C, inset). External alanine application initiates Na^+/alanine exchange (establishing a new equilibrium between T_{out} and the inward-facing configuration, T_{in}; Scheme 1; see appendix). A significantly larger transient current was observed than in the presence of internal K^+, which decayed with a slightly faster time constant of 1.7 ± 0.4 ms (Fig. 5 C). The larger current amplitude in the exchange mode suggests that internal Na^+/alanine is more efficient in driving the binding sites to an outward-facing configuration than intracellular K^+. The faster time constant

indicates that the relaxation rate is now determined by the sum of the rate constants for the bidirectional forward and backward translocation reactions ($k_{obs} = k_1 + k_{-1}$), whereas in the presence of intracellular K^+, only the unidirectional rate constant for forward translocation is observed ($k_{obs} = k_{-1}$). With $k_1 = 330\ s^{-1}$, we can estimate $k_{-1} = 600\ s^{-1} - 330\ s^{-1} = 270\ s^{-1}$. Therefore, these data suggest that translocation occurs with rates of similar order of magnitude in both directions but with a slight favoring of the inward-facing configuration at 0 mV.

We also determined the voltage dependence of the transient currents. As shown in Fig. 5 (D and E), the charge movement saturates at very negative transmembrane potentials, but it decreases at positive potentials. This indicates that at $V < -60$ mV, the translocation equilibrium is fully driven toward the inward-facing configuration. The half-maximal potential of about +40 mV confirms the prediction that at 0 mV, the exchange equilibrium is shifted toward the inward-facing configuration.

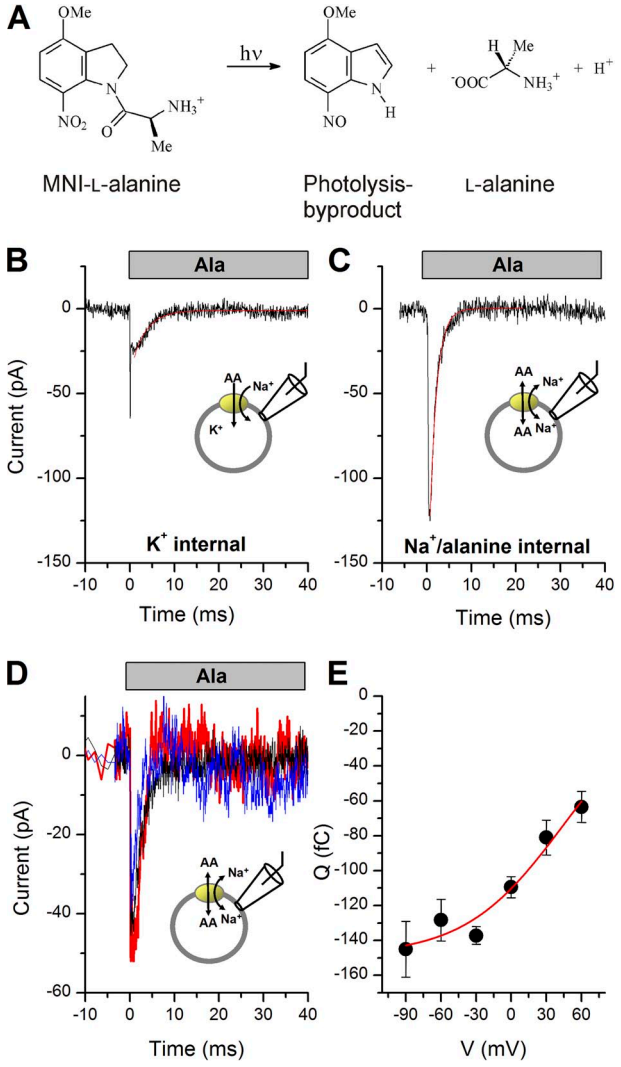

Figure 5. Amino acid exchange is associated with inward charge movement. (A) Mechanism of photolysis of MNI-caged alanine. (B and C) Current in response to liberation of ~200 µM of free alanine from 3 mM of MNI-caged alanine at t = 0 in the presence of internal K^+ (B) or Na^+/alanine (C). The anion was Mes^- in all cases (V = 0 mV). (D) Current response to alanine application at t = 0 at membrane potentials of −60 mV (red), 0 mV (black), and +60 mV (blue). (E) Charge movement as a function of the transmembrane potential. The charge was obtained by integrating the transient current response over time. The red line shows a fit to the Boltzmann equation (see legend to Fig. 3; $z_Q = 0.58$ and $V_Q = 41$ mV).

Amino acid interaction with ASCT2 is electroneutral, but Na^+ interaction is electrogenic

For several Na^+-driven transporters, it was suggested that Na^+ binding and/or conformational changes associated with it contribute to transporter electrogenicity (Loo et al., 1993; Wadiche et al., 1995; Lu and Hilgemann, 1999; Watzke et al., 2001; Forster et al., 2002). We tested this possibility by measuring current responses to voltage jumps in the absence of extracellular amino acid, restricting ASCT2 to reaction steps associated with Na^+ binding. As shown in Fig. 6 A (left), transient, inhibitor-sensitive currents were observed upon stepping the membrane potential from 0 to −60 or +60 mV when the extracellular [Na^+] was 0.5 mM. A concentration of 0.5 mM was chosen because it is close to the K_m of the empty transporter for Na^+ (K_{Na1}), which was in the 0.05- and 0.5-mM range, dependent on the various methods used to determine this value. At [Na^+] = K_m, the maximum charge movement should be observed. In contrast, at saturating [Na^+], no or little charge movement should be observed, because the jump to more negative voltage cannot drive additional Na^+ into the already occupied binding site. Consistent with this expectation, no currents were observed at 140 mM of external Na^+, when the Na^+-binding site(s) is fully saturated (Fig. 6 A, right). The charge movement was capacitive in nature, with the charge of the off-response being of equal magnitude but of opposite sign of that of the on-response (Fig. 6 A). The voltage dependence of the charge movement could be represented with the Boltzmann equation, yielding an apparent valence, z_Q, of 0.41 ± 0.1 (Fig. 6 B). Collectively, these results indicate that Na^+ binding, or a conformational change induced by this binding, is electrogenic. The results also confirm the existence of a high affinity Na^+-binding site with an apparent affinity in the submillimolar range.

We next tested whether the PB computations predict voltage dependence of Na^+ binding. The models were based on the movement of a Na^+ ion from the water phase ($\varepsilon = 80$) to one of the three predicted, occluded Na^+-binding sites, respectively. The calculated valences are shown in Fig. 6 D. These valences are positive (Table S2), as expected for movement of a positively charged ion into the low dielectric environment of the protein. These

computational results support our experimental results on electrogenic Na^+ association. The actual Na^+ association process may be separated into two steps. First, Na^+ may move into its binding site through an aqueous access channel in a voltage-independent fashion. Second, occlusion of the bound Na^+ results in charge displacement. This possibility is supported by MD simulations shown in Fig. S3, demonstrating that the Na1 site becomes hydrated from the extracellular side in the absence of any bound Na^+. Therefore, it is likely that the main electrogenic step is the occlusion of the Na^+ in its binding site after initial electroneutral binding through an aqueous pathway.

The amino acid substrate presumably binds to ASCT2 in its zwitterionic form. Although the overall charge of the substrate is zero, the positive and negative charges on the amino and carboxy group may lead to transmembrane charge movement. However, the K_m of ASCT2 for alanine was independent of the transmembrane potential (Fig. 6 C). Furthermore, PB calculations indicate that alanine binding is associated with little valence ($z = 0.04$; Fig. 6 D; see illustration of setup in the inset). Therefore, it is likely that the amino acid association reaction is electroneutral.

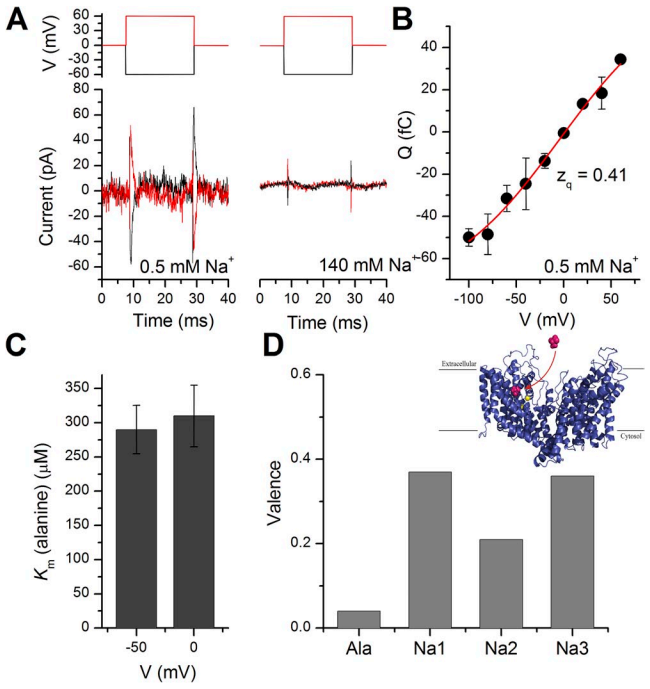

Figure 6. Na^+ binding to the empty transporter is electrogenic, but alanine binding is electroneutral. (A) Currents in response to voltage jumps (top panel indicates voltage protocol) at 0.5 mM of extracellular Na^+ (left) and 140 mM Na^+ (right) (counterion was Mes^-). The intracellular solution contained 120 mM NaMes/10 mM alanine. (B) Voltage dependence of the charge movement of the on-response (solid line represent fit to a Boltzmann equation). (C) Voltage dependence of the K_m of ASCT2 for alanine. The intracellular solution contained 120 mM NaSCN/10 mM alanine, and the extracellular solution contained 140 mM NaMes. (D) Predicted valences computed by PB analysis for alanine binding as well as for the binding of Na^+ to three hypothesized binding sites. The inset shows an illustration of the alanine-binding reaction used for calculation of the valence.

Evidence for conserved Na^+ sites from MD simulations

A high resolution crystal structure is available for the aspartate transporter GltPh (Boudker et al., 2007), which is highly homologous to ASCT2. Although the overall ASCT2 sequence shares only 30% identity and 50% similarity with GltPh, the critical C-terminal transport domain is much better conserved with 45% identity and 66% similarity. The amino acid residues within 4 Å of the ligand-binding site are even better conserved, with 69% identity and 85% similarity. Therefore, we hypothesize that an ASCT2 homology model based on the GltPh structure will provide a reasonable starting point for MD simulations, at least for the transmembrane domain, while keeping in mind the caveats associated with MD simulations of low resolution or homology models.

We first studied the transporter with bound amino acid (alanine) and with two Na^+ ions in the sites that are analogous to the Na1 and Na2 sites of GltPh (see Fig. S2 for an illustration of the simulation setup). After 8 ns of simulation, the alanine molecule, as well as the two Na^+ ions, remained in their binding sites (Fig. 7, A and B). Reentrant loop 2 (RL2) adapted to the lower molecular volume of the bound alanine compared with aspartate in GltPh, resulting in a closing in of the alanine molecule and exclusion of water in a lid-like fashion. These results suggest that the function of RL2 as the external gate that protects the bound amino acid from the water phase is conserved in ASCT2. The Na^+ ion in the Na2 site is coordinated by a total of five main chain carbonyl oxygens from the SVGA motif at the tip of RL2 (SIGT in GltPh), as well as from the TVN motif in TM7 (TIN in GltPh), which show 86% similarity between ASCT2 and GltPh (Fig. 7 B). The Na1 site is formed by the two carboxylate side chain oxygens of D473, as well as the main chain and side chain oxygens of N384 and two other main chain carbonyls from TM8 (Fig. 7 A).

Both Na^+ ions were stable in their predicted binding sites in the 2 Na^+/alanine-loaded transporter within the 8 ns of simulation, as shown for Na2 in Fig. 7 C (red trace; $n = 3$). The sodium ion in the Na1 site also remained stable in the absence of occupation of the Na2 site, as well as when both amino acid and Na^+ in the Na2 site were absent (Fig. 7 D). Stability is indicated by a lack of significant variability of the D473(Oδ)-Na1 distance with time. This result indicates that occupation of the Na1 site can occur in the empty transporter, i.e., in the absence of bound amino acid substrate. In contrast, a sodium ion in the Na2 site was only stable when the amino acid was bound (Fig. 7 C). In the absence of alanine, the cation dissociated from the Na2 site within 8 ns in two out of three simulation runs (representative traces shown in Fig. 7 C; black line shows dissociating cation).

This result suggests that the cation in the Na2 site is only stable in the presence of bound amino acid.

In some MD simulations, the sodium ion in the Na1 site became coordinated by an oxygen atom in the carboxylate side chain of D386. This configuration is analogous to an intermediate cation site proposed by Huang and Tajkhorshid (2010) for GltPh. This finding raises the possibility that a third Na^+-binding site exists, in which the Na^+ is coordinated by the D386 side chain as well as by the T139 side chain oxygen from TM3. Evidence for the existence of such a site has been obtained by previous mutagenesis studies showing that neutralization of D386 resulted in a dramatic reduction of Na^+ affinity of ASCT2 (Tao et al., 2006), as well as MD simulations of glutamate transporters (Huang and Tajkhorshid, 2010; Heinzelmann et al., 2011; Bastug et al., 2012). Therefore, we placed a third sodium ion in the proposed Na3 site and performed MD simulations. The third Na^+ ion in the site analogous to the GltPh Na3 site was stable within 8 ns of simulation (Fig. 7, E and F). These results indicate the potential for a third Na^+-binding site on ASCT2. It should be noted that Larsson et al. (2010) have proposed an alternative Na3 site in the related glutamate transporters. Because there have been no mutational studies on this site for ASCT2, we have not analyzed it further.

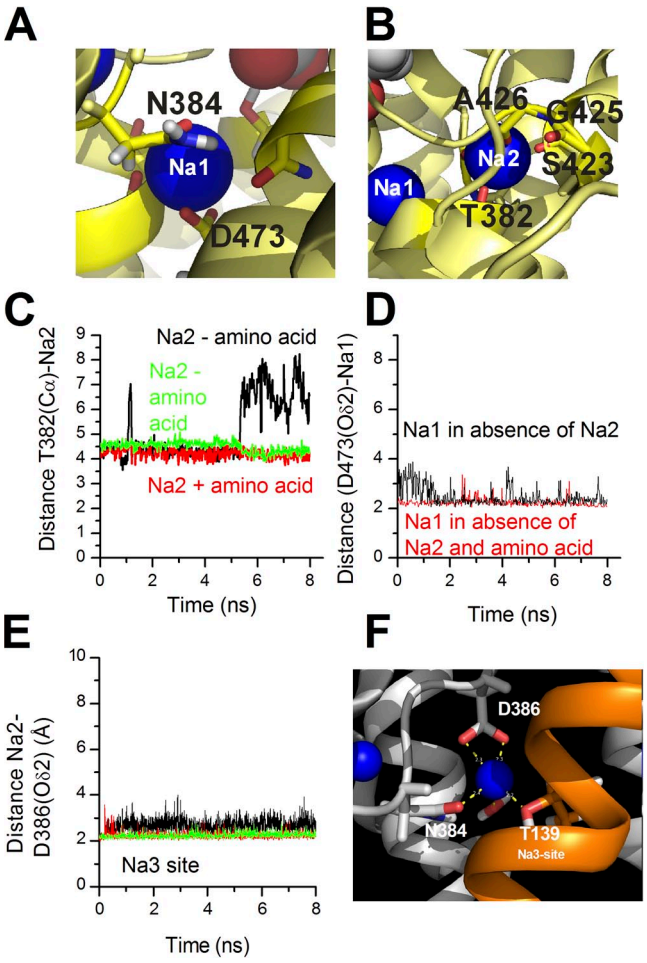

Figure 7. Sodium-binding sites are conserved in ASCT2. (A and B) Na1 (A)- and Na2 (B)-binding sites for Na^+ after 8 ns of MD simulation. (C) Representative traces for the distance between the T382 α carbon and the Na^+ ion in the Na2 site as a function of time for the alanine- and Na1-bound transporter (red), and in the absence of alanine (black and green). (D) Time evolution of the distance between D473(Oδ2) and the cation in the Na1 site in the absence of occupied Na2 (black), as well as in the absence of both Na2 and alanine (red). (E) Distances calculated from an 8-ns MD simulation between D386(Oδ2) and Na3. The colors indicate distances calculated from the same simulation in the three different subunits (black, chain A; red, chain B; green, chain C). (F) Predicted Na3-binding site at the end of a 10-ns simulation.

DISCUSSION

In this paper, we have used a combined experimental and computational approach to determine the mechanism and electrogenicity of Na^+ interaction with and translocation by the neutral amino acid exchanger ASCT2. The two major conclusions from these studies are the following: (1) Despite being an electroneutral exchanger, Na^+-coupled amino acid translocation by ASCT2 is electrogenic and, thus, sensitive to the transmembrane potential. (2) In contrast to previous suggestions, amino acid exchange is coupled to the translocation of at least two but possibly three Na^+ ions. Cation and amino acid binding to ASCT2 is sequential, with at least one Na^+ binding to the *apo*, empty form of the transporter, followed by amino acid binding, followed by binding of another Na^+ to the substrate-bound form (Fig. 4 E).

Overall, the mechanism of amino acid transport by ASCT2 is surprisingly similar to the mechanism of glutamate transport by the related glutamate transporters from the SLC1 family (Wadiche and Kavanaugh, 1998; Watzke et al., 2001; Bergles et al., 2002). Like in the glutamate transporters, amino acid transport requires the cotransport of two to three sodium ions. The sequence of sodium and amino acid binding also appears to be conserved between the ASCT and excitatory amino acid transporter (EAAT) members of the family, as are the major amino acids that contribute oxygen ligands to the cation-binding sites. Finally, Na^+ binding to the empty transporter, or conformational changes associated with it, is associated with charge movement in ASCT2. Similar findings, based on voltage-jump analysis, were reported for several subtypes of EAATs (Wadiche et al., 1995; Watzke et al., 2001).

Despite these similarities, there are also significant differences between the neutral and acidic amino acid transporters of the SLC1 family. First, Na^+ binds to the empty ASCT2 with very high apparent affinity in the submillimolar range (this work and Grewer and Grabsch, 2004). In contrast, the affinity of the *apo* form of EAATs for Na^+ is low, with an apparent affinity of 100 mM for

excitatory amino acid carrier 1 (EAAC1; Tao et al., 2006). The high affinity is important for ASCT2's physiological function as an amino acid exchanger, because the tightly bound sodium ion most likely never dissociates from the transporter (Bröer et al., 2000). Although the intracellular affinity for Na^+ is not known, it is most likely high, such that Na^+ has a modulatory function rather than providing a driving force for substrate transport. Second, ASCT2, in contrast to the EAATs, cannot complete a full transport cycle because intracellular K^+ is unable to drive relocation of the empty transporter, as also noted in Bröer et al. (2000). Clearly, no steady-state component of the transport current was observed in the presence of intracellular K^+ (Fig. 3 A), indicating that net forward transport of amino acid is not possible, or is at least slow. Furthermore, internal Na^+/amino acid are much more capable of rearranging the binding sites to outward-facing than K^+ (Fig. 3, A and B). Collectively, these results suggest that K^+ is not able to interact with ASCT2. The preference of Na^+ over K^+ may be caused by the high Na^+ affinity of ASCT2, preventing intracellular K^+ from displacing Na^+, despite its ~30-fold higher intracellular concentration. It is noteworthy that the potentially negatively charged glutamate residue, E373 in EAAC1, is substituted by a glutamine in ASCT2 (Q392). E373 has been implicated in potassium interaction as well as in protonation of the glutamate transporter (Pines et al., 1995; Grewer et al., 2003). A transporter with the E373Q mutation is defective in potassium-induced relocation and is pH insensitive. ASCT2 is also pH insensitive (Grewer et al., 2003), suggesting that the glutamine side chain can mimic a protonated glutamic acid residue. If this hypothesis is correct, electrostatic charge compensation in position in ASCT2 is unchanged compared with the protonated glutamate transporter.

Our results from the concentration-jump analysis directly show that inward amino acid translocation by ASCT2 is coupled to the inward movement of positive charge. These results agree well with the valence calculations from solving the linearized PB equation, predicting a positive valence for the fully loaded transporter. Because the bound amino acid is zwitterionic, but net neutral, the translocated charge could be generated by positive charges of the bound Na^+ ions, by positively charged ion/substrate-binding sites, or by both of these effects. However, according to the PB calculations, the empty, unloaded transporter either carries net negative charge in the binding sites (negative valence) or is neutral, providing evidence that the observed inward charge movement is caused by inward movement of the cotransported Na^+ ions within the membrane electric field.

In a previous report by Bussolati et al. (1992), L-threonine transport by natively expressed system ASC was found to be weakly voltage dependent, with a bell-shaped dependence of flux on voltage. If influx of amino acid takes place only by exchange, a bell-shaped voltage dependence of uptake is expected, as either the forward or reverse rate becomes rate limiting at extreme membrane potentials (see Appendix for a simplified mathematical treatment). Similar considerations have been put forward for electroneutral but voltage-dependent Na^+ exchange by the Na/K ATPase (De Weer et al., 1988). The slight favoring of inward transport over outward transport of alanine at 0 mV is expected to result in a slight left shift of the maximum of the flux–voltage relationship to positive potentials (see Fig. A1 in Appendix).

Our new results allow us to extend previous mechanistic models proposed for amino acid exchange by ASCTs and system ASC (Bussolati et al., 1992; Bröer et al., 2000). The extended model (Fig. 8) includes a Na^+/amino acid stoichiometry of at least 2:1, with sequential binding of Na^+ and amino acid. The first Na^+ ion binds to the *apo* state of the transporter in a voltage-dependent manner, or it elicits a voltage-dependent conformational change. The second possibility is more likely, because the MD simulations predict that Na^+ accesses its Na1 site through a water-filled channel, which upon binding closes while excluding water molecules from the binding site. Therefore, the overall cation-binding reaction probably includes an initial electroneutral Na^+ association process through an aqueous environment, followed by electrogenic occlusion of the cation through water exclusion. The function of this first Na^+-binding step is modulatory because the high affinity of the transporter for this sodium presumably prevents dissociation from the transporter. It should be noted that we do not know yet the affinity for Na^+ of the inward-facing transporter. However, based on the predicted modulatory function of this Na^+-binding site, this affinity is expected

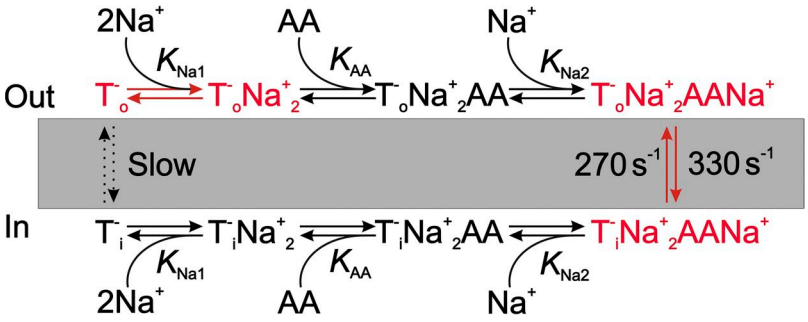

Figure 8. Extended mechanism for amino acid transport by ASCT2. The rate constants for the exchange equilibrium were estimated from Fig. 3 and are given for alanine as the amino acid substrate. The Na^+/substrate dissociation sequence on the intracellular side is speculative and not based on experimental data. Electrogenic reactions are illustrated in red.

to be high. In fact, the K_m of the transporter for extracellular alanine is not significantly changed when the intracellular [Na^+] is lowered from 140 to 10 mM (K_m = 160 ± 50 µM; unpublished data). Therefore, 10 mM of cytosolic [Na^+] is still saturating the internal Na^+-binding site.

Binding of the first Na^+ ion is most likely followed by binding of another Na^+ to the empty transporter, resulting in a doubly Na^+-bound transporter. Both MD simulations and experimental data support the existence of a second Na^+-binding site on the amino acid–free transporter, although this evidence is less strong than for the first cation-binding step. The Na_2-bound transporter subsequently binds the amino acid substrate in an electroneutral fashion, followed by association with a third Na^+ ion. The MD results clearly show that this ion, which is expected to bind to the Na2 site, is unstable in the absence of bound amino acid, suggesting that amino acid binding is a prerequisite for closure of RL2. An occupied Na2 site may further stabilize the closed RL2, but Na^+ binding to the Na2 site by itself is clearly not sufficient to stabilize the closed RL2. Overall, this mechanism is in excellent agreement with models on sequential Na^+/substrate binding to the EAATs (Watzke et al., 2001; Huang and Tajkhorshid, 2008, 2010), suggesting that these aspects of the transport mechanism are conserved within the SLC1 family.

The pre–steady-state kinetic data suggest that amino acid translocation by ASCT2 is fast, occurring on a millisecond time scale. From these data, a maximum exchange rate at optimum voltage for alanine of ∼150–200 s^{-1} is estimated (see Appendix), although the existence of slower electroneutral steps that are not seen in our experiments cannot be fully excluded. These results suggest that ASCT2 can release or take up amino acids rapidly, as required if it is involved in processes such as the glutamate–glutamine cycle (Bröer et al., 1999; Deitmer et al., 2003), which recycles the neurotransmitter glutamate in the brain. In contrast to the exchange reaction, the conformational changes of the empty transporter are probably slow. However, the data shown in Fig. 3 A suggest that the rate of rearrangements of the empty transporter, although slow, is nonzero because some of the amino acid–binding sites are facing the extracellular side even in the absence of ions that can promote outward translocation (K^+ inside). Despite this ability of the empty transporter to rearrange binding sites, this process is physiologically not significant because it is too slow to support measurable transport.

ASCT2, as a transporter of the amino acid glutamine, is expressed in many tissues, including the brain (Bröer and Brookes, 2001). It was proposed to be involved in the glutamate–glutamine cycle (Bröer and Brookes, 2001), which recycles the excitatory neurotransmitter glutamate. Recently, ASCT2 has also been shown to be up-regulated in rapidly growing tumor cells, and its knockout led to a reduction in cell growth (Fuchs and Bode, 2005; Nicklin et al., 2009). Therefore, our results may assist in the understanding of the function of ASCT2 in its physiological environment as well as under pathophysiological conditions.

Conclusions

In this paper, we demonstrate that an overall electroneutral amino acid exchanger can mediate voltage-dependent amino acid transport through transmembrane charge movement of the amino acid translocation reaction. The molecular basis of the charge movement in the translocation step is the cotranslocation of two to three positively charged Na^+ ions with the zwitterionic, neutral amino acid. This finding is in contrast to previous reports, predicting coupling of amino acid transport to a single cotransported Na^+ ion. The fully loaded complex bears positive charge, resulting in charge movement associated with the amino acid translocation process. However, electroneutral translocation steps may also exist. Binding of the Na^+ ions is modulatory because of the high affinity of the Na^+-binding sites.

APPENDIX

For the following simplified one-step amino acid exchange process,

$$T_{out} \underset{k_{-1}}{\overset{k_1}{\rightleftarrows}} T_{in}, \qquad \text{(SCHEME 1)}$$

the unidirectional rate for amino acid influx, J_1, can be written as:

$$J_1 = N_t \frac{k_1 k_{-1}}{k_1 + k_{-1}}. \qquad (2)$$

Here, N_t is the total number of transporters in the membrane. The voltage dependence of flux can then be derived by using the theoretical expressions for the voltage dependence of the forward and reverse rate constants:

$$J_1(V) = N_t \frac{k_1(0)e^{-zFV/RT} k_{-1}(0)e^{zFV/RT}}{k_1(0)e^{-zFV/RT} + k_{-1}(0)e^{zFV/RT}}. \qquad (3)$$

Here, V is the membrane potential; z is the valence; and F, R, and T have their usual meaning. This equation represents a bell-shaped curve when plotted as a function of the voltage. The voltage of the maximum flux can be obtained by finding the voltage at which the first derivative is zero:

$$0 = N_t \frac{-k_1(0)k_{-1}(0)\,[k_1(0)ze^{-zFV/RT} k_{-1}(0)ze^{zFV/RT}]}{[k_1(0)e^{-zFV/RT} + k_{-1}(0)e^{zFV/RT}]^2}. \qquad (4)$$

Solving this equation for V yields the expression:

$$V_{max} = \frac{-\log(k_1(0)/k_{-1}(0))}{2z}. \quad (5)$$

As expected, the V_{max} is 0 when the forward and backward rate constants are identical. If the valence, z, is positive, the maximum shifts to more positive potentials with increasing forward rate constant, a situation that would be consistent with our kinetic data and the voltage dependence of threonine flux determined by Bussolati et al. (1992). This effect is illustrated in Fig. A1, assuming a valence of ±0.5.

Derivation of the equation for the [Na+] dependence of the anion current

The total population of anion-conducting states, $\overline{TNa^+}$ and $\overline{TAlaNa_2^+}$, according to the kinetic scheme in Fig. 2, is:

$$P = \frac{[Na^+](K_{Na2}K_s + r[Na^+][S])}{K_{Na2}K_s(K_{Na1}+[Na^+]) + [Na^+][S](K_{Na2}+[Na^+])}. \quad (6)$$

Here, K_{Na1} and K_{Na2} are the intrinsic dissociation constants for Na^+, as illustrated in Fig. 2 (bottom scheme), K_S is the intrinsic dissociation constant for the substrate, and r accounts for the ratio of conductances of the $\overline{TAlaNa_2^+}$ over the $\overline{TNa^+}$ state.

At saturating alanine concentration, the total current then becomes:

$$I_{total} = I_{max}(\text{saturating alanine}) + I_0(\text{no alanine}) \quad (7)$$

$$= -\frac{[Na^+]}{(K_{Na1}+[Na^+])} + r\frac{[Na^+]}{(K_{Na2}+[Na^+])}. \quad (8)$$

The equations for the apparent dissociation constant for alanine, K_m, as a function of Na^+ have been derived by us in Watzke et al. (2001):

$$K_m = K_S \cdot \left(\frac{K_{Na1}+[Na^+]}{[Na^+]}\right) \cdot \left(\frac{K_{Na2}}{K_{Na2}+[Na^+]}\right). \quad (9)$$

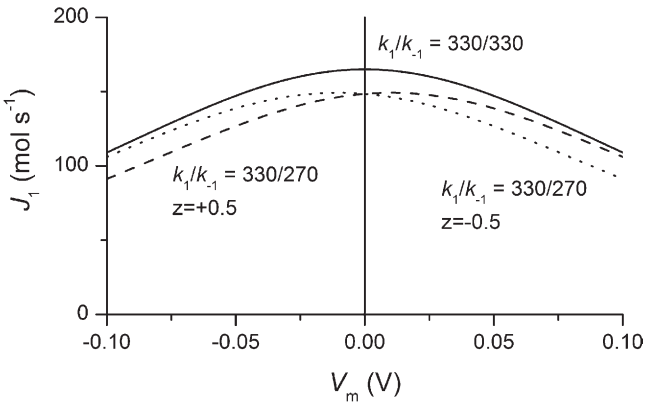

Figure A1. Simulation of the voltage dependence of flux according to Eq. 3.

In case of two Na^+ ions binding before the amino acid, the apparent K_m is:

$$K_m = K_S \cdot \left(\frac{K_{Na1}+[Na^+]}{[Na^+]}\right)^2. \quad (10)$$

We are grateful to Dr. Stefan Bröer for helpful comments regarding the manuscript.

This work was supported by the National Institutes of Health (grant 2R01NS049335-06A1 to C. Grewer) and Binational Science Foundation (grant 2007051 to C. Grewer and Baruch I. Kanner).

Lawrence G. Palmer served as editor.

Submitted: 10 December 2012
Accepted: 22 April 2013

REFERENCES

Albers, T., W. Marsiglia, T. Thomas, A. Gameiro, and C. Grewer. 2012. Defining substrate and blocker activity of alanine-serine-cysteine transporter 2 (ASCT2) ligands with novel serine analogs. *Mol. Pharmacol.* 81:356–365. http://dx.doi.org/10.1124/mol.111.075648

Baker, N.A., D. Sept, S. Joseph, M.J. Holst, and J.A. McCammon. 2001. Electrostatics of nanosystems: application to microtubules and the ribosome. *Proc. Natl. Acad. Sci. USA.* 98:10037–10041. http://dx.doi.org/10.1073/pnas.181342398

Bastug, T., G. Heinzelmann, S. Kuyucak, M. Salim, R.J. Vandenberg, and R.M. Ryan. 2012. Position of the third Na+ site in the aspartate transporter GltPh and the human glutamate transporter, EAAT1. *PLoS ONE.* 7:e33058. http://dx.doi.org/10.1371/journal.pone.0033058

Bergles, D.E., A.V. Tzingounis, and C.E. Jahr. 2002. Comparison of coupled and uncoupled currents during glutamate uptake by GLT-1 transporters. *J. Neurosci.* 22:10153–10162.

Bode, B.P. 2001. Recent molecular advances in mammalian glutamine transport. *J. Nutr.* 131:2475S–2485S.

Boudker, O., R.M. Ryan, D. Yernool, K. Shimamoto, and E. Gouaux. 2007. Coupling substrate and ion binding to extracellular gate of a sodium-dependent aspartate transporter. *Nature.* 445:387–393. http://dx.doi.org/10.1038/nature05455

Bröer, A., N. Brookes, V. Ganapathy, K.S. Dimmer, C.A. Wagner, F. Lang, and S. Bröer. 1999. The astroglial ASCT2 amino acid transporter as a mediator of glutamine efflux. *J. Neurochem.* 73:2184–2194.

Bröer, A., C. Wagner, F. Lang, and S. Bröer. 2000. Neutral amino acid transporter ASCT2 displays substrate-induced Na+ exchange and a substrate-gated anion conductance. *Biochem. J.* 346:705–710. http://dx.doi.org/10.1042/0264-6021:3460705

Bröer, S., and N. Brookes. 2001. Transfer of glutamine between astrocytes and neurons. *J. Neurochem.* 77:705–719. http://dx.doi.org/10.1046/j.1471-4159.2001.00322.x

Bussolati, O., P.C. Laris, B.M. Rotoli, V. Dall'Asta, and G.C. Gazzola. 1992. Transport system ASC for neutral amino acids. An electroneutral sodium/amino acid cotransport sensitive to the membrane potential. *J. Biol. Chem.* 267:8330–8335.

Callenberg, K.M., O.P. Choudhary, G.L. de Forest, D.W. Gohara, N.A. Baker, and M. Grabe. 2010. APBSmem: a graphical interface for electrostatic calculations at the membrane. *PLoS ONE.* 5:e12722. http://dx.doi.org/10.1371/journal.pone.0012722

Choudhary, O.P., R. Ujwal, W. Kowallis, R. Coalson, J. Abramson, and M. Grabe. 2010. The electrostatics of VDAC: implications for selectivity and gating. *J. Mol. Biol.* 396:580–592. http://dx.doi.org/10.1016/j.jmb.2009.12.006

Crisman, T.J., S. Qu, B.I. Kanner, and L.R. Forrest. 2009. Inward-facing conformation of glutamate transporters as revealed by their

inverted-topology structural repeats. *Proc. Natl. Acad. Sci. USA.* 106:20752–20757. http://dx.doi.org/10.1073/pnas.0908570106

Darden, T., D.M. York, and L. Pedersen. 1993. Particle mesh Ewald: an N log(N) method for Ewald sums in large systems. *J. Chem. Phys.* 98:10089–10092. http://dx.doi.org/10.1063/1.464397

De Weer, P., D.C. Gadsby, and R.F. Rakowski. 1988. Overview: stoichiometry and voltage dependence of the Na/K pump. *Prog. Clin. Biol. Res.* 268A:421–434.

Deitmer, J.W., A. Bröer, and S. Bröer. 2003. Glutamine efflux from astrocytes is mediated by multiple pathways. *J. Neurochem.* 87:127–135. http://dx.doi.org/10.1046/j.1471-4159.2003.01981.x

Eswar, N., B. John, N. Mirkovic, A. Fiser, V.A. Ilyin, U. Pieper, A.C. Stuart, M.A. Marti-Renom, M.S. Madhusudhan, B. Yerkovich, and A. Sali. 2003. Tools for comparative protein structure modeling and analysis. *Nucleic Acids Res.* 31:3375–3380. http://dx.doi.org/10.1093/nar/gkg543

Forster, I.C., K. Köhler, J. Biber, and H. Murer. 2002. Forging the link between structure and function of electrogenic cotransporters: the renal type IIa Na+/Pi cotransporter as a case study. *Prog. Biophys. Mol. Biol.* 80:69–108. http://dx.doi.org/10.1016/S0079-6107(02)00015-9

Fuchs, B.C., and B.P. Bode. 2005. Amino acid transporters ASCT2 and LAT1 in cancer: partners in crime? *Semin. Cancer Biol.* 15:254–266. http://dx.doi.org/10.1016/j.semcancer.2005.04.005

Grabe, M., H. Lecar, Y.N. Jan, and L.Y. Jan. 2004. A quantitative assessment of models for voltage-dependent gating of ion channels. *Proc. Natl. Acad. Sci. USA.* 101:17640–17645. http://dx.doi.org/10.1073/pnas.0408116101

Grewer, C., and E. Grabsch. 2004. New inhibitors for the neutral amino acid transporter ASCT2 reveal its Na+-dependent anion leak. *J. Physiol.* 557:747–759. http://dx.doi.org/10.1113/jphysiol.2004.062521

Grewer, C., N. Watzke, T. Rauen, and A. Bicho. 2003. Is the glutamate residue Glu-373 the proton acceptor of the excitatory amino acid carrier 1? *J. Biol. Chem.* 278:2585–2592. http://dx.doi.org/10.1074/jbc.M207956200

Grewer, C., Z. Zhang, J. Mwaura, T. Albers, A. Schwartz, and A. Gameiro. 2012. Charge compensation mechanism of a Na+-coupled, secondary active glutamate transporter. *J. Biol. Chem.* 287:26921–26931. http://dx.doi.org/10.1074/jbc.M112.364059

Groeneveld, M., and D.J. Slotboom. 2010. Na(+):aspartate coupling stoichiometry in the glutamate transporter homologue Glt(Ph). *Biochemistry.* 49:3511–3513. http://dx.doi.org/10.1021/bi100430s

Heinzelmann, G., T. Baştuğ, and S. Kuyucak. 2011. Free energy simulations of ligand binding to the aspartate transporter Glt(Ph). *Biophys. J.* 101:2380–2388. http://dx.doi.org/10.1016/j.bpj.2011.10.010

Huang, Z., and E. Tajkhorshid. 2008. Dynamics of the extracellular gate and ion-substrate coupling in the glutamate transporter. *Biophys. J.* 95:2292–2300. http://dx.doi.org/10.1529/biophysj.108.133421

Huang, Z., and E. Tajkhorshid. 2010. Identification of the third Na+ site and the sequence of extracellular binding events in the glutamate transporter. *Biophys. J.* 99:1416–1425. http://dx.doi.org/10.1016/j.bpj.2010.06.052

Humphrey, W., A. Dalke, and K. Schulten. 1996. VMD: visual molecular dynamics. *J. Mol. Graph.* 14:33–38. http://dx.doi.org/10.1016/0263-7855(96)00018-5

Larsson, H.P., X. Wang, B. Lev, I. Baconguis, D.A. Caplan, N.P. Vyleta, H.P. Koch, A. Diez-Sampedro, and S.Y. Noskov. 2010. Evidence for a third sodium-binding site in glutamate transporters suggests an ion/substrate coupling model. *Proc. Natl. Acad. Sci. USA.* 107:13912–13917. http://dx.doi.org/10.1073/pnas.1006289107

Loo, D.D., A. Hazama, S. Supplisson, E. Turk, and E.M. Wright. 1993. Relaxation kinetics of the Na+/glucose cotransporter. *Proc. Natl. Acad. Sci. USA.* 90:5767–5771. http://dx.doi.org/10.1073/pnas.90.12.5767

Lu, C.C., and D.W. Hilgemann. 1999. GAT1 (GABA:Na^+:Cl^-) cotransport function. Steady state studies in giant Xenopus oocyte membrane patches. *J. Gen. Physiol.* 114:429–444. http://dx.doi.org/10.1085/jgp.114.3.429

Mim, C., Z. Tao, and C. Grewer. 2007. Two conformational changes are associated with glutamate translocation by the glutamate transporter EAAC1. *Biochemistry.* 46:9007–9018. http://dx.doi.org/10.1021/bi7005465

Mwaura, J., Z. Tao, H. James, T. Albers, A. Schwartz, and C. Grewer. 2012. Protonation state of a conserved acidic amino acid involved in Na(+) binding to the glutamate transporter EAAC1. *ACS Chem Neurosci.* 3:1073–1083. http://dx.doi.org/10.1021/cn300163p

Nicklin, P., P. Bergman, B. Zhang, E. Triantafellow, H. Wang, B. Nyfeler, H. Yang, M. Hild, C. Kung, C. Wilson, et al. 2009. Bidirectional transport of amino acids regulates mTOR and autophagy. *Cell.* 136:521–534. http://dx.doi.org/10.1016/j.cell.2008.11.044

Phillips, J.C., R. Braun, W. Wang, J. Gumbart, E. Tajkhorshid, E. Villa, C. Chipot, R.D. Skeel, L. Kalé, and K. Schulten. 2005. Scalable molecular dynamics with NAMD. *J. Comput. Chem.* 26:1781–1802. http://dx.doi.org/10.1002/jcc.20289

Pines, G., Y. Zhang, and B.I. Kanner. 1995. Glutamate 404 is involved in the substrate discrimination of GLT-1, a (Na+ + K+)-coupled glutamate transporter from rat brain. *J. Biol. Chem.* 270:17093–17097. http://dx.doi.org/10.1074/jbc.270.29.17093

Reyes, N., C. Ginter, and O. Boudker. 2009. Transport mechanism of a bacterial homologue of glutamate transporters. *Nature.* 462:880–885. http://dx.doi.org/10.1038/nature08616

Rostkowski, M., M.H. Olsson, C.R. Søndergaard, and J.H. Jensen. 2011. Graphical analysis of pH-dependent properties of proteins predicted using PROPKA. *BMC Struct. Biol.* 11:6. http://dx.doi.org/10.1186/1472-6807-11-6

Silva, J.R., H. Pan, D. Wu, A. Nekouzadeh, K.F. Decker, J. Cui, N.A. Baker, D. Sept, and Y. Rudy. 2009. A multiscale model linking ion-channel molecular dynamics and electrostatics to the cardiac action potential. *Proc. Natl. Acad. Sci. USA.* 106:11102–11106. http://dx.doi.org/10.1073/pnas.0904505106

Tao, Z., Z. Zhang, and C. Grewer. 2006. Neutralization of the aspartic acid residue Asp-367, but not Asp-454, inhibits binding of Na+ to the glutamate-free form and cycling of the glutamate transporter EAAC1. *J. Biol. Chem.* 281:10263–10272. http://dx.doi.org/10.1074/jbc.M510739200

Tao, Z., N. Rosental, B.I. Kanner, A. Gameiro, J. Mwaura, and C. Grewer. 2010. Mechanism of cation binding to the glutamate transporter EAAC1 probed with mutation of the conserved amino acid residue Thr101. *J. Biol. Chem.* 285:17725–17733. http://dx.doi.org/10.1074/jbc.M110.121798

Utsunomiya-Tate, N., H. Endou, and Y. Kanai. 1996. Cloning and functional characterization of a system ASC-like Na+-dependent neutral amino acid transporter. *J. Biol. Chem.* 271:14883–14890. http://dx.doi.org/10.1074/jbc.271.25.14883

Valdeolmillos, M., J. García-Sancho, and B. Herreros. 1986. Differential effects of transmembrane potential on two Na+-dependent transport systems for neutral amino acids. *Biochim. Biophys. Acta.* 858:181–187. http://dx.doi.org/10.1016/0005-2736(86)90304-4

Wadiche, J.I., and M.P. Kavanaugh. 1998. Macroscopic and microscopic properties of a cloned glutamate transporter/chloride channel. *J. Neurosci.* 18:7650–7661.

Wadiche, J.I., J.L. Arriza, S.G. Amara, and M.P. Kavanaugh. 1995. Kinetics of a human glutamate transporter. *Neuron.* 14:1019–1027. http://dx.doi.org/10.1016/0896-6273(95)90340-2

Watzke, N., E. Bamberg, and C. Grewer. 2001. Early intermediates in the transport cycle of the neuronal excitatory amino acid carrier EAAC1. *J. Gen. Physiol.* 117:547–562. http://dx.doi.org/10.1085/jgp.117.6.547

Yernool, D., O. Boudker, Y. Jin, and E. Gouaux. 2004. Structure of a glutamate transporter homologue from Pyrococcus horikoshii. *Nature.* 431:811–818. http://dx.doi.org/10.1038/nature03018

Zerangue, N., and M.P. Kavanaugh. 1996a. ASCT-1 is a neutral amino acid exchanger with chloride channel activity. *J. Biol. Chem.* 271:27991–27994. http://dx.doi.org/10.1074/jbc.271.45.27991

Zerangue, N., and M.P. Kavanaugh. 1996b. Flux coupling in a neuronal glutamate transporter. *Nature.* 383:634–637. http://dx.doi.org/10.1038/383634a0

Zhang, Z., G. Papageorgiou, J.E. Corrie, and C. Grewer. 2007. Pre-steady-state currents in neutral amino acid transporters induced by photolysis of a new caged alanine derivative. *Biochemistry.* 46:3872–3880. http://dx.doi.org/10.1021/bi0620860